Evaluating Local Buckling Strength of HSB460 Steel Tubular Columns

Seong-Wook Han[1] · Yeun Chul Park[2] · Ho-Kyung Kim[3,4] · Doobyong Bae[5]

Abstract

High performance steels for bridges (HSB), as adopted by the Korean Design Standard (KDS), having a yield strength greater than 350 MPa have recently been developed. Notably, HSB460, which has a minimum yield strength of 460 MPa, does not exhibit a yield plateau beyond yielding and exhibits strain hardening. Such characteristics could provide advantages by absorbing the greater strain energy of steel members and increasing the local buckling strength, which may help develop more economic bridge designs. However, the current KDS for compression members of steel tubular columns was established based on the results of axial load tests for conventional structural steel having yield strengths from 250 to 350 MPa, which exhibits a yield plateau. Three-dimensional finite element analyses adopting actual stress-strain curve of HSB460 were subsequently carried out to evaluate the buckling strength, by considering the ovality, welding residual stresses, and the cross-section sizes. It was confirmed that HSB460 steel tubular columns could have larger margins compared to the current KDS, primarily due to advantages from strain hardening with no yield plateau. As such, with regards to local buckling, the proposed design guidelines for HSB460 steel is expected to enable a more economic bridge design.

Keywords Steel tubular column · local buckling strength · slenderness · HSB steel · finite element analysis

1 Introduction

High performance steels for bridges (HSB) have recently been developed and subsequently adopted to the Korean Standard (KATS 2018). The advantages of HSB steels are that they have a higher yield strength, higher toughness, and

✉ Yeun Chul Park
ycpark@hnu.kr

1 Department of Infrastructure Safety Research, Korea Institute of Civil Engineering and Building Technology, 283 Goyangdae-Ro, Ilsanseo-Gu, Goyang-Si, Gyeonggi-Do 10223, Republic of Korea

2 Department of Civil and Environmental Engineering, Hannam University, 70 Hannam-ro, Daedeok-gu, Daejeon 34430, Republic of Korea

3 Department of Civil and Environmental Engineering, Seoul National University, 1 Gwanak-ro, Gwanak-gu, Seoul 08826, Republic of Korea

4 Institute of Construction and Environmental Engineering, Seoul National University, 1 Gwanak-ro, Gwanak-gu, Seoul 08826, Republic of Korea

5 School of Civil and Environmental Engineering, Kookmin University, 77, Jeongneung-ro, Seongbuk-gu, Seoul 02707, Republic of Korea
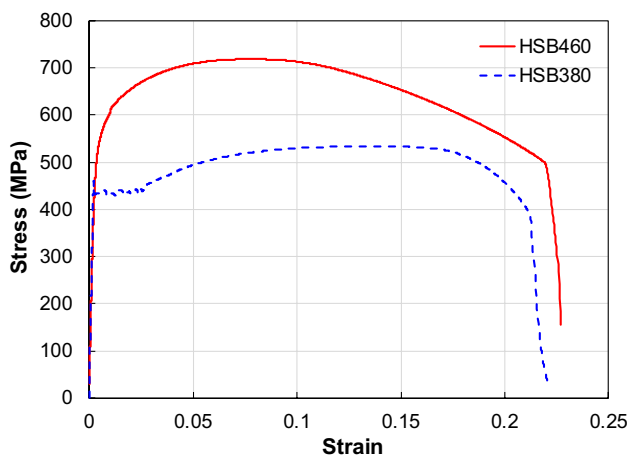
better weldability than conventional structural steels. In particular, the mechanical behavior under axial loading beyond yielding is different. For example, having a yield strength of 460 MPa, HSB460 does not exhibit a yield plateau beyond yielding, and shows strain hardening just after yielding as shown in Fig. 1. Such characteristics provide advantages by potentially increasing resisting forces during plastic deformation, which may result in an economic bridge design. The Korean Society of Steel Construction conducted a research program to propose design guidelines reflecting the characteristics of the HSB steels. As a part of the study, the buckling strength of the steel tubular column for HSB460 steel was investigated.

The current *Korean Design Standard (KDS) 14 31 10* (MOLIT 2016) classifies nonslender-element and slender-element sections of round hollow structural sections (HSS) subject to axial compression as shown in Table 1. In the table, E, D, t, and f_y denote the elastic modulus, tube outer diameter, tube thickness, and yield strength, respectively.

This classification is identical to the design specifications proposed by *ANSI/AISC 360 − 16* (AISC 2016) and *AISI D100-08* (AISI 2008), developed based on compressive test results of steel tubular columns having a yield strength of 250 to 350 MPa (Chen and Ross 1978; Galambos 1998).

Fig. 1 Stress-strain curve of HSB460 compared to HSB380 exhibiting yield plateau

Table 1 Width-to-thickness ratios of round HSS subjected to axial compression in current *KDS 14 31 10* (MOLIT 2016)

Description of sections	Width-to-thickness ratio
Slender-element	$0.11\frac{E}{f_y} < \frac{D}{t} < 0.45\frac{E}{f_y}$
Nonslender-element	$\frac{D}{t} \leq 0.11\frac{E}{f_y}$

As shown in Eq. (1), AISI, as well as KDS and ANSI/AISC, present the local buckling strength f_c of steel tubular columns for both slender and nonslender sections according to the local buckling parameter α, which is $(E/f_y)/(D/t)$.

$$f_c/f_y = \begin{cases} 1.0 & (\alpha \geq 9.1) \\ 0.665 + 0.0368\alpha & (2.27 \leq \alpha \leq 9.1) \end{cases} \quad (1)$$

The local buckling parameter α, which is 9.1 in Eq. (1), corresponds to $0.11E/f_y$, which is the limiting width-to-thickness ratio in Table 1.

Other design guidelines, such as *Eurocode 3* (CEN 2012), *ISO 19,902* (ISO 2007) and *DNVGL-OS-CF101* (DNVGL 2017), specify the local buckling strength in a different form, though all recommend conservatively limiting the width-to-thickness ratio for nonslender-element. For steel having a yield strength of 460 MPa, the width-to-thickness ratio limit for the nonslender-element of these design guidelines is $0.10 E/f_y$, which corresponds to the local buckling parameter of 9.9. Therefore, a thicker tube is required in nonslender-element designs.

The local buckling strengths of the steel tubular columns in current KDS and other specifications have been established based on experimental results using conventional steel. These previous studies indicated that the nonlinearity of the material, i.e., strain hardening, could enhance the structural performance of the column (Gardner and Ashraf 2006; Theofanous et al. 2009; Zhao et al. 2016). Also problematic is that current design specifications not incorporating strain hardening add conservativeness to the design of circular columns. Therefore, it is expected that HSB460 steel could improve the local buckling strength.

In this study, the local buckling strength of hollow steel tubular columns using HSB460 steel was investigated via a three-dimensional (3D) finite element analysis (FEA) to evaluate the effect of strain hardening. The material model incorporated the actual stress-strain curve of HSB460 steel. Next, a parametric study considering various influence variables affecting the buckling strength was conducted. The variables included ovality, welding residual stresses, and the size of the cross-section. The results were then compared with the current KDS, and design guidelines pertaining to the local buckling strength for the hollow steel tubular columns using HSB460 steel were proposed.

2 Finite Element Modelling of Compression Test

The local buckling strength of hollow steel tubular columns using HSB460 steel was evaluated. Commercial FEA software, ABAQUS, was used for the evaluation (Dassualt Systems 2018).

2.1 Material Model of HSB460 Steel

In Fig. 2a, a tensile test for HSB460 steel was conducted according to *ASTM A370* (ASTM 2014). The yield strength of the HSB460 steel according to a 0.2% offset strain was 538 MPa, and the tensile strength was 719 MPa. The stress-strain curve obtained from the test was directly substituted into the finite element model. The finite element model of a tensile test specimen was applied to verify the material model as shown in Fig. 2b. The stress-strain curve in the simulation was in good agreement with the actual stress-strain curve. Since the test was conducted only for tensile loading, it was assumed here that the stress-strain curve for the compression was completely opposite to the tensile stress-strain curve.

2.2 Description of Modelling Steel Tubular Columns

A 3D FEA model was developed to simulate previously conducted compression tests (Chen and Ross 1978; Ostapenko and Gunzelman 1978; Galambos 1998). Prior specimens included hollow tubes having various diameters and thicknesses. Here, to develop local buckling, the lengths of the tubes were limited to twice the diameter. Tubular columns were modeled using a solid element that incorporated eight nodes and reduced integration using an isoparametric
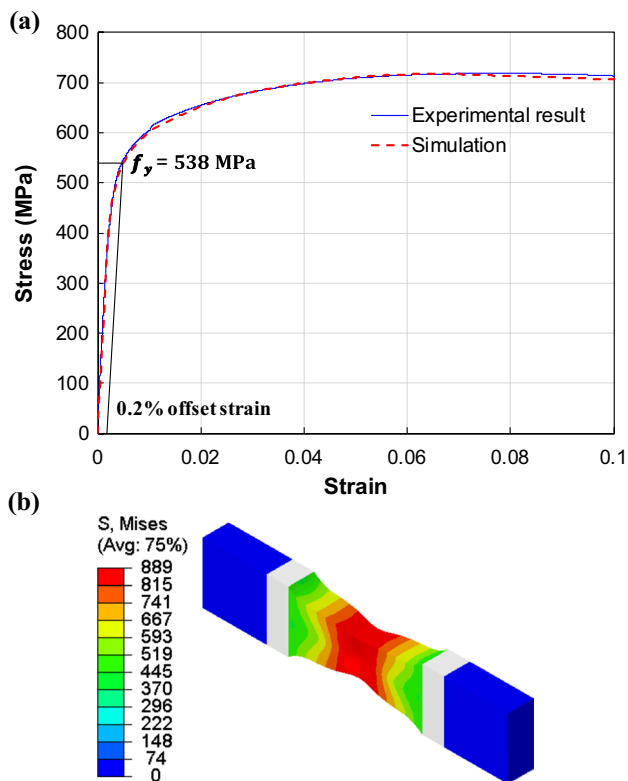
(a)

(b)

Fig. 2 Validation of material model in simulation: (**a**) stress-strain curves of HSB460 steel obtained from tensile test and 3D FEA; and (**b**) 3D FEA model for tensile coupon test

formulation, referred to as C3D8R in ABAQUS. Other than the axial direction of the top surface, both the top and bottom surfaces of the tube were fixed in all directions. Compression was applied as a uniform pressure on the top surface. The local buckling strength was subsequently nonlinearly analyzed using an arc-length method, which can consider the negative stiffness of structures.

Mesh convergence was verified by varying the number of elements along the longitudinal direction. The number of elements in the circumferential and thickness directions were fixed at 188 and 5, respectively; the outer diameter and thickness of the tube were 320 mm and 4.3 mm. In Fig. 3, the normalized buckling strength, i.e., the local buckling strength divided by the yield strength of the 0.2% offset strain, was seen to converge when the number of elements was 40 or more. For subsequent analyses, 120 elements were maintained along the longitudinal direction.

Residual stress in welding could influence the buckling strength of a column. To incorporate the residual stress, the residual stresses measured near a seam weld were collected from several references (Ostapenko and Gunzelman 1975, 1978; Ostapenko and Grimm 1980; Ross 1978). All residual stress measurements were conducted in a longitudinal direction, and distributions of the stresses along the perimeter of
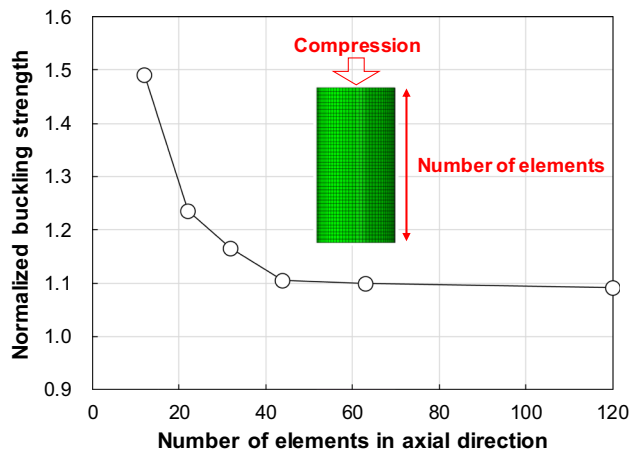

Fig. 3 Results of mesh convergence test

the tubes were recorded as shown in Fig. 4. Near the seam weld, the tensile residual stress is initially seen to be as high as the yield strength, though it rapidly decreased due to compression until reaching equilibrium and disappearing.

Interestingly, the measured residual stresses showed similar distributions along the perimeter regardless of the size of the tubular columns. Diameters of the tubular columns used for the measurements ranged from 380 to 1787 mm. Since the effects of the welding only work locally, the residual stress, regardless of the diameter of the tubular columns, appears to show similar distributions depending on the distance from the seam weld. In the finite element model, the residual stress was distributed by dividing the columns into seven zones based on distance from the seam weld and considering the self-equilibrium as shown in Fig. 4.

Ovality can be caused by the manufacturing process or by installation in the field. Thus, the ovality of the cross section was also considered as an initial geometric imperfection of
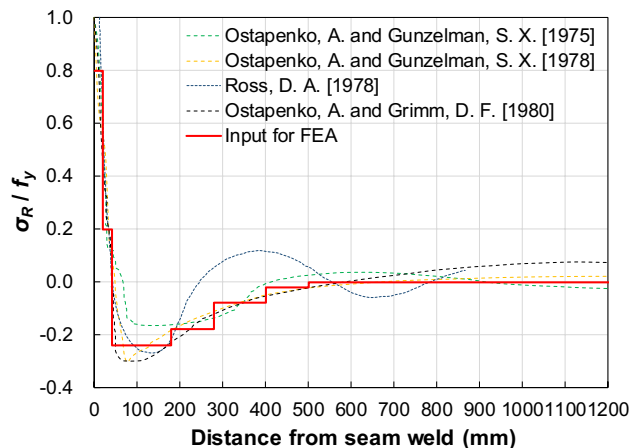

Fig. 4 Distributions of residual stress near the seam weld

the tubular column. To simulate the ovality, the cross-section was assumed to be an ellipse, and is defined as follows.

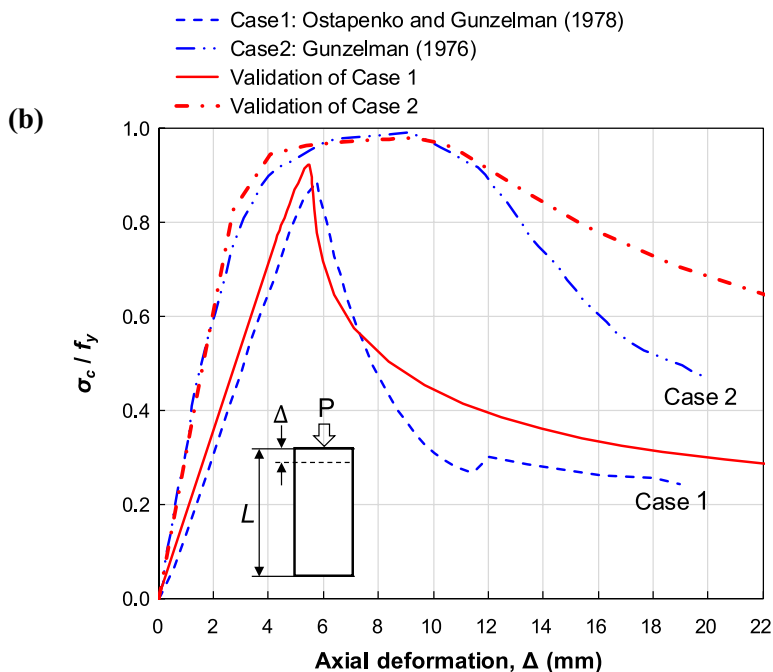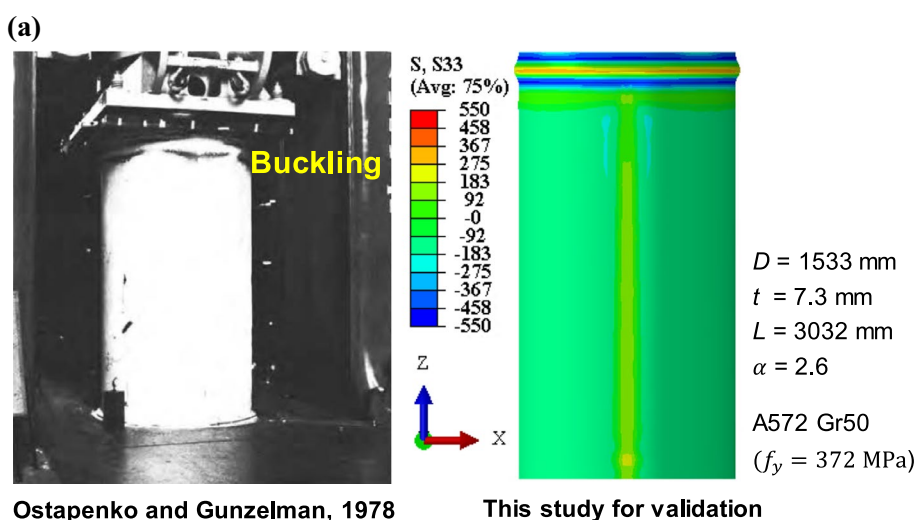$$\text{Ovallity} = \frac{D_{max.} - D_{min.}}{D_{avg.}} \tag{2}$$

where D_{max} and D_{min} are the maximum and minimum outer diameters of the cross-section, respectively, and D_{avg} is the average of the maximum and minimum outer diameters.

2.3 Validation of 3D Finite Element Model

To validate the model, compression tests for the tubular columns that were performed by Gunzelman (1976) and Ostapenko and Gunzelman (1978) were simulated as shown in Fig. 5. The first column made with ASTM A572 Gr. 50 steel (ASTM 2018) had an outer diameter (*D*), thickness (*t*), and length (*L*) of 1533 mm, 7.3 mm, and 3032 mm, respectively (Ostapenko and Gunzelman 1978). The local buckling parameter α of this column was 2.6, indicating a slender section. Another column had a relatively nonslender section, with a local buckling parameter of 7.5 (Gunzelman 1976). The second column was also made with ASTM A572 Gr. 50 steel (ASTM 2018), and had an outer diameter, thickness, and length of 717 mm, 8.349 mm, and 2050 mm, respectively. The finite element models displayed a round cross-section and incorporated a residual stress distribution, as discussed in the previous section.

Fig. 5 Validation of the FEA model: (**a**) photo of compression test; and (**b**) comparing results of experiment and 3D FEA

(a)

Ostapenko and Gunzelman, 1978   This study for validation

$D = 1533$ mm
$t = 7.3$ mm
$L = 3032$ mm
$\alpha = 2.6$

A572 Gr50
($f_y = 372$ MPa)

(b)

- - - Case1: Ostapenko and Gunzelman (1978)
- ‧‧ Case2: Gunzelman (1976)
—— Validation of Case 1
—‧— Validation of Case 2

In Fig. 5a, local buckling occurred near the top surface, and a similar buckling mode was observed by Ostapenko and Gunzelman (1978). Compressive stress normalized by the yield strength was then plotted for the axial displacement at the loading point as shown in Fig. 5b. Compressive stress almost linearly increased with respect to the axial deformation until reaching the maximum. After reaching the maximum, local buckling immediately started, such that the axial deformation rapidly increased even though the compressive stress decreased. A similar behavior was observed in both experiments. Notably, the maximum compressive stress, i.e., the local buckling strength, differed by only 3% for both simulations.

3 Influence of Ovality and Residual Stress on Buckling Strength

3.1 Ovality

The influence of ovality on the local buckling strength was first examined. The tubular columns can become oval from the manufacturing process or due to installation process in the field. According to KDS, the maximum allowable ovality is 1.5%. Thus, local buckling strengths of tubular columns having 0 and 1.5% ovality were compared as shown in Fig. 6. The outer diameter of the tubular columns was 320 mm, and no residual stress was incorporated. The width-to-thickness ratio was varied by changing the thickness.

The results showed that the local buckling strength (f_c) normalized by the measured yield strength (f_y) increased as the local buckling parameter was increased and approached approximately 1.1. Regardless of the width-to-thickness ratio, however, the influence of ovality on the local buckling strength was minor as the maximum ovality of 1.5% was
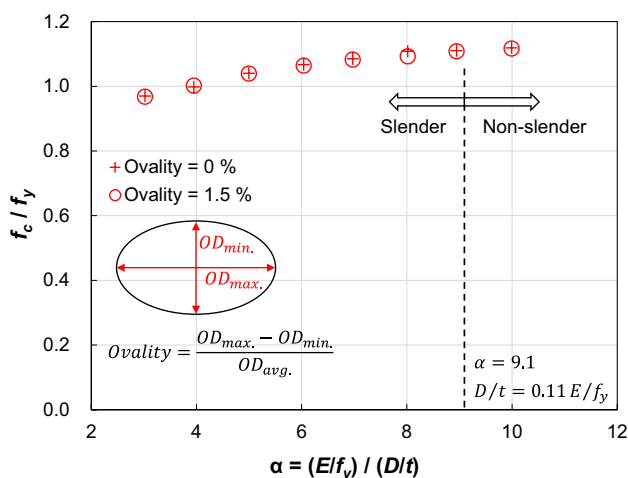
set not to reduce the buckling strength. If the ovality was increased, the buckling strength could decrease. Therefore, the analysis results demonstrated the validity of limiting ovality to 1.5%, based on experimental specifications.

3.2 Residual Stress

As explained above, residual stress in the longitudinal direction varies significantly along the perimeter. In Fig. 5a, local buckling in the tubular column occurs in the form of out-of-plane bending at the tube wall. Therefore, residual stress in the longitudinal direction could affect the local buckling strength. To further examine the influence of residual stress, tubular columns having two extreme outer diameters, 320 mm and 1920 mm, were examined. Local buckling strengths of the tubular columns were then evaluated according to the presence of residual stress as shown in Fig. 7.

In the figure, the local buckling strengths of tubular columns having a large diameter or not incorporating the residual stress in the model were almost the same. However, the local buckling strengths significantly decreased for tubular columns having a small diameter and residual stress. These results are due to the fact that the area occupied by high tensile residual stress is relatively larger, as shown in Fig. 8.

Figure 8 presents the residual stress distribution for two different sizes, though with the identical local buckling parameters α of 6. The smaller column has an outer diameter (D), thickness (t), and length (L) of 320 mm, 5.2 mm and 640 mm, respectively. The size of the larger column is six times larger than that of the smaller column. The red area in the figure highlights the region in which the residual stress is close to the tensile yield stress, which is 538 MPa. Since the distribution of the residual stress is determined by the distance from the seam weld, a larger portion is seen
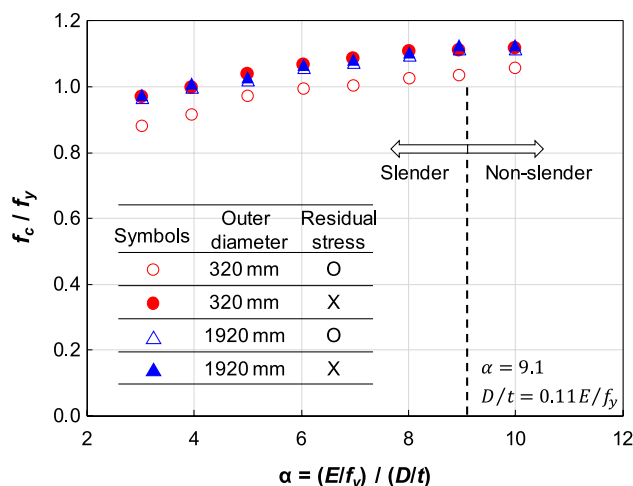
Fig. 6 Dependency of ovality on the local buckling strength

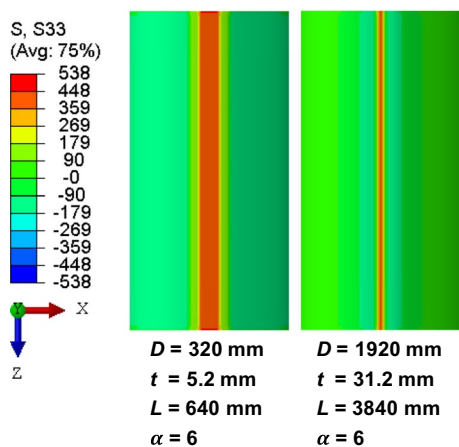**Fig. 7** Dependency of residual stress and column dimensions on local buckling strength

Fig. 8 Comparing residual stress distributions of tubular columns having outer diameters of 320 mm and 1920 mm

to be under high tensile stress. Therefore, a smaller tubular column was deemed to be more vulnerable to local buckling due to its out-plane bending.

4 Local Buckling Strength of HSB460 Steel

Results of the analysis were compared to the current design standard in order to evaluate advantages of tubular columns of HSB460 steel, with regards to the local buckling strength.

4.1 Proposal of Design Equation for the Local Buckling Strength of HSB460 Steel

In Fig. 9, local buckling strengths considering the residual stress were compared to the KDS specification, which is
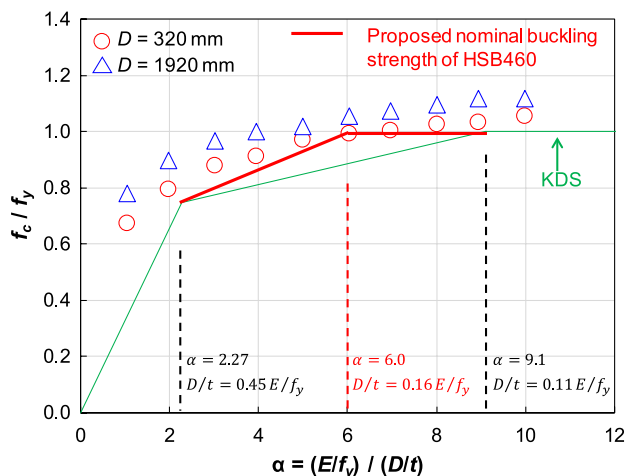
identical to the current AISI. Buckling strengths of all cases were significantly greater than for KDS. The current KDS suggests that the nominal local buckling strength is the same as the yield strength when the local buckling parameter α is greater than 9.1, which is the lower limit of the nonslender-element. When HSB460 steel was used, however, the local buckling strength was greater than the yield strength when the local buckling parameter α was greater than 6.0. Considering the advantage of the HSB460 steel, the local buckling parameter for nonslender HSB460 tubular column could actually be lowered to 6.0.

This result indicates that the limit for the width-to-thickness ratio for the nonslender-element could be increased from $0.11\,E/f_y$ to $0.16\,E/f_y$, which corresponds to a local buckling parameter of 6.0. Therefore, an approximately 45% thinner tubular column could be considered as a nonslender-element. Considering this advantage of HSB460 steel, Eq. (3) defines the nominal local buckling strength of steel tubular columns using HSB460 steel.

$$f_c/f_y = \begin{cases} 1.0 & (\alpha \geq 6.0) \\ 0.596 + 0.0674\alpha & (2.27 \leq \alpha \leq 6.0) \end{cases} \quad (3)$$

4.2 Advantage of HSB460 Steel with Regards to Local Buckling Strength

Axial compressive stress with respect to the axial deformation was plotted to investigate why HSB460 steel displays greater local buckling strength as shown in Fig. 10. The outer diameter (D) and thickness (t) of the tubular column were 320 mm and 5.2 mm, respectively. Thus, the local buckling parameter α was 6.0, which exhibited a local buckling strength equal to the yield strength. Overall, the behavior of
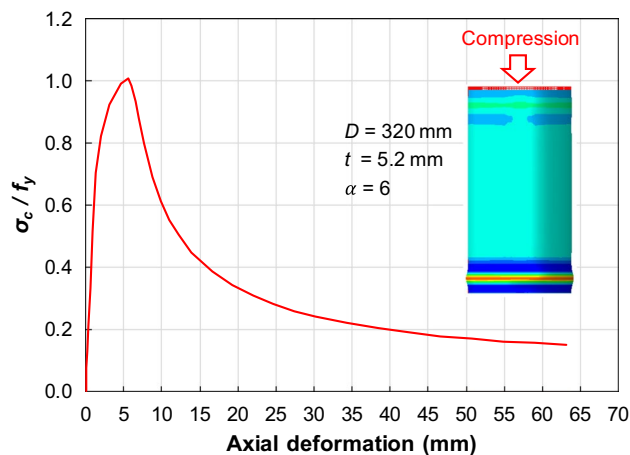

Fig. 9 Comparison of current local buckling strengths of steel tubular columns recommended by KDS and HSB460 steel

Fig. 10 Variation of compressive stress with respect to axial deformation (HSB460 steel)
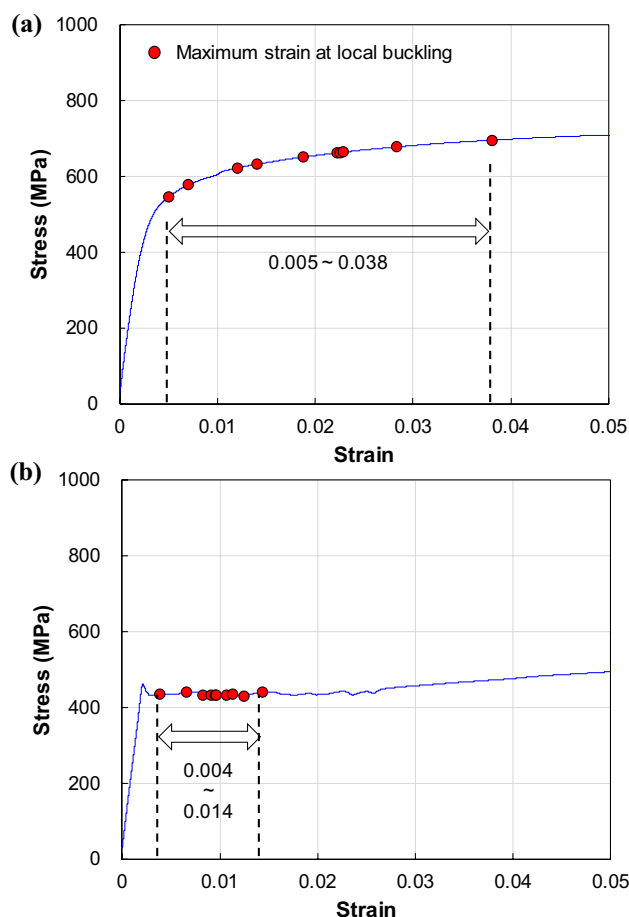
Fig. 11 Range of compressive strain when local buckling occurs: (**a**) HSB460 steel; and (**b**) HSB380 steel

the tubular column using HSB460 steel was similar to that of conventional steel shown in Fig. 5b. However, a slight difference was observed in that the compressive stress did not linearly increase as the stress approached the yield strength. Rather, the slope of the curve gradually decreased until the compressive stress reached the maximum.

The difference in curves was due to the stress-strain behavior after yielding. In Fig. 9, maximum strains when local buckling occurred were in the range of 0.5 to 3.8%. In Fig. 1, when the material was changed to HSB380 steel the maximum strains were the range of 0.4–1.4% for the same sizes of tubular columns.

Figure 11a and b present the stress-strain curves of HSB460 and HSB380 steels, respectively. When the local buckling of HSB460 steel occurred, the maximum strains were in the region of strain hardening. In contrast, the maximum strains of HSB380 steel were in the region of the yield plateau. When the yield plateau exists, strain increases without additional stress. Thus, local buckling occurs when the compressive stress reaches the yield strength of the material. However, HSB460 steel does not exhibit a yield plateau

beyond yielding, rather, it shows strain hardening after yielding. In other words, HSB460 steel can acquire additional strain energy after yielding due to strain hardening. Therefore, local buckling occurs at stresses greater than the yield strength of the material, resulting in greater local buckling strength and the current conservative design specifications.

5 Conclusions

Compression tests of tubular columns were simulated using 3D FEA by incorporating the stress-strain relationship of HSB460 steel obtained from tensile coupon tests. Local buckling strengths of the HSB460 steel tubular columns were evaluated by considering ovality, welding residual stresses, and the cross-section size. It was found that residual stresses in the longitudinal direction significantly reduced the buckling strength of tubular columns having smaller diameters and thicknesses. For tubular columns having larger diameters and thicknesses, however, the effect of residual stress was relatively minor because the area occupied by high tensile residual stress was smaller. In addition, ovality was found to have little influence on the buckling strength.

HSB460 steel was confirmed to exhibit a greater local buckling strength compared to the current KDS. The advantage of HSB460 steel was due to strain hardening beyond yielding, without exhibiting a yield plateau. Consequently, the buckling strength of an HSB460 steel tubular column has a larger margin compared to the current KDS. As a result, using HSB460 steel, the current limit for the width-to-thickness ratio for nonslender elements could be increased by approximately 45%, such that thinner tubular columns could be considered as a nonslender-element.

Based on this investigation, a new nominal local buckling strength design guideline for HSB460 steel could be proposed. The proposed design guideline, however, was established based on FEA results. To further revise the current design specifications, however, these analysis results should be validated by additional experiments.

References

AISI. (2008). *AISI D100-08 The cold-formed steel design manual*. Washington, DC: American Iron and Steel Institute.

AISC. (2016). *ANSI/AISC 360 – 16: Specification for structural steel buildings*. Chicago: American Institute of Steel Construction.

ASTM. (2014). *ASTM Standard A370-14: Standard test methods and definitions for mechanical testing of steel products*. West Conshohocken: ASTM International.

ASTM. (2018). *ASTM Standard A572/A572M-18: Standard specification for high-strength low-alloy columbium-vanadium structural steel*. West Conshohocken: ASTM International.

CEN. (2012). *Eurocode 3: Design of steel structures - Part 1–1: General rules and rules for buildings*.

Chen, W. F., & Ross, D. A. (1978). Tests of fabricated tubular columns. *Fritz Laboratory Reports. Paper 478*. Bethlehem, PA, USA: Lehigh University.

Dassault Systemes. (2018). *ABAQUS 2018*. Providence: Dassault Systemes Simulia Corp.

DNVGL. (2017). *Offshore Standard DNVGL-OS-CF101: Design of offshore steel structures, general - LRFD method*. Høvik: Det Norske Veritas Germanischer Lloyd.

Galambos, T. V. (1998). *Guide to stability design criteria for metal structures*. Hoboken: Wiley.

Garnder, L., & Ashraf, M. (2006). Structural design for non-linear metallic materials. *Engineering Structures, 28,* 926–934.

Gunzelman, S. X. (1976). Experimental local buckling of fabricated high-strength steel tubular columns. *Fritz Laboratory Reports. Paper 2174*. Bethlehem, PA, USA: Lehigh University.

ISO. (2007). *ISO 19902: Petroleum and natural gas industries—Fixed steel offshore structures*. Genève: International Organization for Standardization.

KATS. (2018). *KS D 3868: Rolled steels for bridge structures*. Sejongsi: Korean Agency for Technology and Standards. (in Korean).

MOLIT. (2016). *Korean Design Standard (KDS) 14 31 10: Design Standard for Steel Structural Members (LRFD)*. Sejong-si, Republic of Korea: Ministry of Land, Infrastructure and Transport (in Korean).

Ostapenko, A., & Grimm, D. F. (1980). Local buckling of cylindrical tubular columns made of a-36 steel. *Fritz Laboratory Reports. Paper 2234*. Bethlehem, PA: Lehigh University.

Ostapenko, A., & Gunzelman, S. X. (1975). Local buckling tests on two high-strength steel tubular columns. *Fritz Laboratory Reports. Paper 2172*. Bethlehem, PA: Lehigh University.

Ostapenko, A., & Gunzelman, S. X. (1978). Local buckling tests on three steel large-diameter tubular columns. Paper presented at the *4th International Specialty Conference on Cold-Formed Steel Structures*.

Ross, D. A. (1978). The strength and behavior of fabricated tubular steel columns. *Ph.D. dissertation*. Bethlehem, PA: Lehigh University.

Theofanous, M., Chan, T. M., & Gardner, L. (2009). Structural response of stainless steel oval hollow section compression members. *Engineering structures, 31*, 922–934.

Zhao, O., Gardner, L., & Young, B. (2016). Structural performance of stainless steel circular hollow sections under combined axial load and bending—Part 2: Parametric studies and design. *Thin-Walled Structures, 101,* 240–248.